

A.D. Short^a, R.M. Ambrosi^a, A.A. Wells^a, D.N. Burrows^b, J.E. Hill^b, J.A. Nousek^b,
G. Tagliaferri^c, G. Chincarini^c, O. Citterio^c

^aPhysics & Astronomy Department, University of Leicester, UK. ^bDepartment of Astronomy & Astrophysics, Penn State University, US. ^cOsservatorio Astronomico di Brera, Milano, Italy

The Swift Observatory is due for launch in September 2003. It carries a wide field Burst Alert Telescope (BAT) and two narrow field instruments, the UV and Optical Telescope (UVOT) and the X-Ray Telescope (XRT). The configuration and performance of the XRT are reported in an accompanying paper [1]. Here, we report on the status of the XRT calibration, including the mechanism adopted for generating the response matrix.

Swift XRT End to End Calibration

The Swift XRT detector, filter and mirror optics have been calibrated independently at unit level. These data have been combined and used to predict XRT performance [3] and to verify the method adopted for response matrix generation. However, the true performance of the telescope, operating in its various modes will only be established through end to end testing in the Panter X-ray facility in Germany. This testing will also provide the data which is required in order to produce the baseline instrument response matrices.

Panter Calibration Objectives

The formal objectives of the XRT calibration are...

1. Focus check
2. PSF calibration
3. Verify centroiding performance
4. Measure effective area
5. Measure count rate linearity
6. Measure spectral response

Panter Calibration X-ray Data Set

In order to meet the calibration test objectives, X-ray data will be accumulated at...

- 5 energies (277, 1487, 4511, 6404 and 8048eV)
- 12 values of flux (using 4 instrument modes)
- on axis and 4 off axis angles in both y and z directions plus special tests of...

- automatic transition between modes
- timing measurement using chopper
- axial rotation to establish gravity effects

giving a total of 176 files with a minimum statistical requirement of 5000 photons per file. Assuming a maximum data taking efficiency of 50%, this will take at least 5 days (24 hour working).

Response Matrix Generation

It is only possible to obtain calibration data at discrete photon energies. Therefore, in order to generate the response across the energy band, a suitable model is required which can be tuned to fit the measured calibration data. Historically, a normalised combination of two or more gaussians was often an adequate representation of the spectral redistribution (rmf) and measured efficiency terms (CCD quantum efficiency (QE), filter transmission and mirror effective area) would be combined in the auxiliary response (arf). However, in the case of the Swift (and XMM) detectors, simply combining gaussians is not a satisfactory means of fitting the spectral redistribution, because the low energy response of the CCD is enhanced and non-gaussian detector features are significant. For Swift we will generate the rmf using a monte carlo simulation of X-ray detection in the CCD. This model also gives us a CCD QE curve which we fit to measured QE and then use to generate the arf.

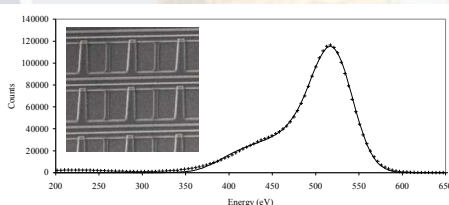


Fig 2. Spectral re-distribution. Calibration data (points) and model (line). Asymmetric surface losses are significant due to "open" electrode structure (inset)

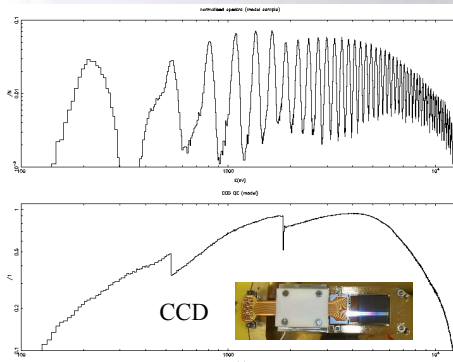


Fig 3. Upper panel: A subset of simulated energy channels. Lower panel: By simulating all channels and dividing by the number of photons simulated we obtain the CCD QE.

The model is then run for all 4096 energy channels in order to produce the response matrix which includes the CCD quantum efficiency by default. Multiplying through by the filter transmission and mirror effective area gives a combined rmf-arf. However, for Swift, we normalise the rmf and extract the CCD QE (figure 3) so that it may be combined with the filter transmission and mirror effective area in a separate arf which is more traditional.

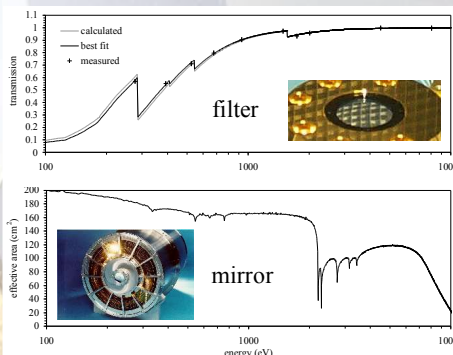


Fig 4. Upper panel: Measured and modelled optical blocking filter transmission. Lower panel: Measured mirror effective area.

The transmission of the optical blocking filter (480Å Al on 1700Å polyimide) and the effective area of the grazing incidence optics are shown in figure 4. By combining these with the CCD QE we obtain the XRT effective area (arf) shown in figure 5.

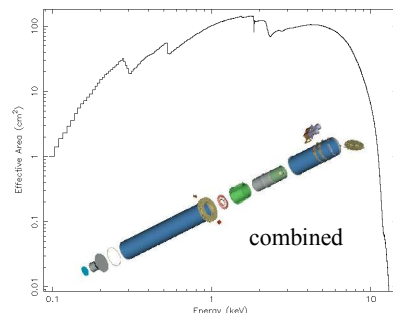


Fig 5. Preliminary total effective area and response matrix (inset) of the Swift XRT

For more information contact A.D. Short: adts@star.le.ac.uk



Fig 1. The Panter facility operated by the Max-Planck-Institut für extraterrestrische Physik (MPE)

Panter Facility

The Panter facility has the following key characteristics.

- 123m beam-line. Chamber cycle time typically 2 days
- Numerous X-ray sources. We will use discrete fluorescence sources with monochromators as appropriate
- Choppers available for timing analysis and flux reduction
- Flux monitored at source and target down to ~5 photons/cm²/s at the telescope aperture
- Filaments available at the source and in the chamber for off axis optical contamination and light tightness testing
- Theta/phi table allows off axis measurements to ±3°
- Integration area better than class 1000 environment
- Contamination monitoring in the facility with mass spectrometers and QCMs

The XRT CCD has an open electrode structure [2,4,5,6] (figure 2 inset) which increases the low energy quantum efficiency. However, low energy X-rays absorbed close to the electrode structure suffer a degree of charge loss which is a function of both interaction depth and position within the pixel. A simple surface loss function has therefore been incorporated into a monte carlo simulation of X-ray detection in the CCD which also includes electrode transmission, photo-electric absorption, escapes & fluorescence, charge generation, charge cloud spreading, mapping to pixels, charge transfer, electronic noise and event reconstruction.

The monte carlo code is applied in several ways. First a looped version is used to simulate single energies and perform least squares best fitting to cleaned and normalised mono-energetic calibration spectra. In this way the best fit model parameters are found for different regions of the energy band.

1. Tagliaferri G., et al. Proceedings this meeting
2. Turner, M.J.L., et al. 2000 A&A 365, L27-L35

3. Short, A.D. et al. 2002 proc woods hole (in print)
4. Short, A.D., et al. 1998 SPIE 3445, L13-27

5. Short, A.D., et al. 2002 NIM A 484 211-224
6. Hiraga, J., et al. 2001 NIM A, 465, L384-393